

# Multi-temporal intensity and coherence analysis of SAR images for land cover change detection on the Island of Crete

E. Nikolaeva<sup>1</sup>, O. Sykioti<sup>1</sup>, P. Elias<sup>1</sup>, C. Kontoes<sup>1</sup>

<sup>1</sup>National Observatory of Athens; Institute for Astronomy, Astrophysics, Space Applications & Remote Sensing

## ABSTRACT

This study presents the use of multi-temporal Synthetic Aperture Radar (SAR) images for detection of land cover changes in the eastern part of the Island of Crete (Greece). For this purpose, fourteen Envisat ASAR acquisitions from July 2004 to December 2006 were calibrated and registered.

We applied a temporal filter and spatial averaging to the backscatter intensity to reduce the noise. Furthermore, we used the concept that the changes between different backscatter intensity observations can show changes on the target dielectric properties. In order to detect changes due to geometrical characteristics of land cover types, we created coherence maps using twenty-seven interferometric pairs with proper spatial and temporal baselines. In all calculations, layover and shadow effects, as well as the sea, were masked by using information from the digital elevation model of the area. The observed changes in the coherence values were analyzed with respect to different decorrelation factors that can contribute to the loss of coherence.

Our results present the different backscatter values for several land cover types (farmland, olive groves, forests, etc.). In addition, some land cover types such as olive groves show variations of backscatter signal due to the density and height of trees. Furthermore, olive groves show good coherence in interferograms with short time intervals. All interferometric pairs have low coherence in farmland because of the rapid growth of plants. Finally, the maps of backscatter temporal changes and coherence changes were superimposed and compared to auxiliary data such as multi-temporal optical satellite imagery (i.e. Landsat/ETM, Terra/Aqua MODIS) and thematic land cover maps (Corinne 2000). We found that changes are mostly due to plant growth and man-made activity.

This ongoing study shows the potential of SAR in providing complementary information such as changes in dielectric and geometric properties to optical data in land cover dynamics monitoring.

## INTRODUCTION

Starting in 1991 the ERS-1 satellites with a radar system on board began to make measurements of the surface of the Earth. Nowadays different space agencies have a huge archive of the radar data at various frequencies and covering the whole Earth [1].

Multi-temporal Synthetic Aperture Radar (SAR) images have been used for observation and monitoring of different dynamic processes such as hazard-related landscape changes due to natural or human-caused activity [2]. SAR

images include information about the intensity and phase of the backscattered signal. These two measurements may be used in different ways, such as detection of deformation based on phase differences [3] or land cover classification and change by utilizing the intensity and phase [4]. Several research results have shown the usefulness of SAR contribution to map vegetation cover and monitor changes in forest environments [5]. In addition, the combination of phase and intensity can reveal reliable information about land cover changes, which may not be evident in the intensity alone [6]. The radar backscatter signal is a complex parameter and depends on the interplay of many factors.

Generally, the radar backscatter from vegetation is defined by various parameters from both the canopy/target and the sensor characteristics. The canopy/target parameters that determine the backscatter are the canopy structure (size, orientation, and distribution of scattering surfaces within the canopy such as trunks, branches and foliage), the surface roughness and slope (relative to wavelength) [2], the dielectric constant (moisture content) and the angle/orientation of the canopy/target.

The primary scatterers in a tree canopy are elements (leaves, branches, and stems) with a size on the order of the wavelength or larger and an orientation similar to that of the incoming signal polarization. Elements smaller than the wavelength produce little backscatter but can attenuate the signal.

Moreover, the backscatter signal is influenced by the amount of moisture content in the canopy and the underlying soil [7], [8] by means of the dielectric constant. A saturated vegetation canopy has a high dielectric value and therefore is a strong reflector and reduces the radar signal penetration through the canopy. On the other hand, dry canopy has a low dielectric constant and a low radar reflectivity. For this reason, the backscatter information can be useful for investigating canopy and soil moisture changes.

On the other hand, the sensor characteristics that determine the backscatter are the wavelength/frequency (in general, the longer the system's wavelength, the higher is the capability of the signal to penetrate the vegetation canopy), the polarization (HH, VV, or HV), the incidence angle [7], [8] (shallower incidence angle signals have a stronger interaction with the canopy) and the spatial resolution.

Despite of all the above conditions, the multi-temporal variation of radar backscatter is recommended as a classifier to map land cover types due to the good calibration of radar data [5]. In particular, multi-temporal C-band data are well-suited to monitor forested areas due to the low temporal changes of forest [5]. In contrast, agricultural/farmland areas may be detected in C-band as the area with large temporal changes due to plant growth [9]. Also, C-band can reveal differentiations between forest and other types of vegetation covers [5].

This study has two main objectives. Changes are traced in the mean backscatter value and in both intensity and phase by calculation of the absolute complex covariance of the complex radar images.

The application are is the eastern part of the Island of Crete. Multi-temporal Envisat ASAR data are used for the study of the island's main vegetation types in two processing steps. First, we differentiate vegetation types by using multi-temporal SAR intensity and then investigate the spatial and temporal variation in the vegetation intensity on the eastern part of the Island of Crete. In the second step, we map a vegetated surface such as farmland using extracted information from the coherence map which is decorrelated within a few days due to growth [10], [11].

## STUDY AREA

The area selected for this study is the eastern part of the Island Crete (Fig. 1). Crete is the largest island in Greece and the fifth largest island in the Mediterranean Sea. It is located in the southern part of the Aegean Sea separating the Aegean from the Libyan Sea. It is a mountainous island, with deep valleys and gorges. The climate is a consistent Mediterranean climate with dry, hot summers and mild damp winters. However, the weather can suddenly change due to frequent and sometimes strong winds. The annual precipitation is low (not higher than 1400 mm per year) and it rains on average 65 days per year (<http://www.kreta-umweltforum.de/>).

The Mediterranean climate has a significant impact on the vegetation of the island. There are dominant wild and cultivated olive groves, marquis shrublands, sclerophyll forests and oak in the Island. The land cover and land use types in this region can be classified into olive groves, sclerophyll, wood-shrubs, conifers, farmland, according to Corine Land Cover map (2000).

For the backscatter analysis, we have selected the five most common vegetation types (olive groves, sclerophyll, coniferous, wood-shrub, farmland) as data samples across the study area. The locations of data samples are shown in Figure 1. Each sample polygon covers only a single land cover type. Samples are properly selected in order to be subject to the same illumination and topographical conditions (slope aspect and orientation). In all the cases, the slope angles do not exceed  $30^{\circ}$  and the elevation range is from 300 to 450 meters. The area of sampling polygons varies between  $27 \text{ m}^2$  and  $675 \text{ m}^2$ .

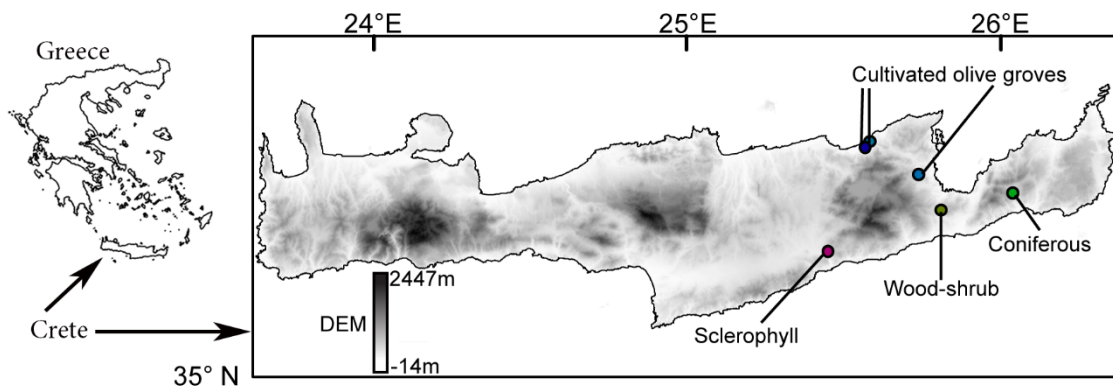


Figure 1. Greece and location of the Island Crete. Background image is ASTER DEM 30 meters resolution. Location of sample polygons: sclerophyll, wood-shrub, coniferous, cultivated olive groves are shown.

## DATA AND METHODS

We used fourteen C-band (microwave frequency of 5.6 cm) Envisat ASAR images in the ascending pass of the satellite spanning July 2004 to December 2006 (see Table 1). [5]. Despite the time sparsity of the data, both the leaf-on and leaf-off seasons are covered.

Furthermore, auxiliary data such as multi-temporal optical satellite imagery (Landsat/ETM and Terra/Aqua MODIS) and the Corine Land Cover map 2000 (CLC2000 with spatial resolution 100m) provide classification of the land cover and were utilized in this study. The slope angle and aspect were calculated by using the 30 meter resolution ASTER Digital Elevation Model (DEM). These two calculations were applied to estimate possible terrain effects on the SAR data. Precipitation information on the study area was retrieved from the ground meteorological station in Heraklion airport.

| Satellite/Sensor | Year | Month | Day |
|------------------|------|-------|-----|
| Envisat/ASAR     | 2004 | Jul   | 2   |
| Envisat/ASAR     | 2004 | Aug   | 6   |
| Envisat/ASAR     | 2004 | Sep   | 10  |
| Envisat/ASAR     | 2004 | Oct   | 15  |
| Envisat/ASAR     | 2004 | Dec   | 24  |
| Envisat/ASAR     | 2005 | Jan   | 28  |
| Envisat/ASAR     | 2005 | Apr   | 8   |
| Envisat/ASAR     | 2005 | Jul   | 22  |
| Envisat/ASAR     | 2005 | Aug   | 26  |
| Envisat/ASAR     | 2005 | Nov   | 4   |
| Envisat/ASAR     | 2006 | Feb   | 17  |
| Envisat/ASAR     | 2006 | Mar   | 24  |
| Envisat/ASAR     | 2006 | Nov   | 24  |
| Envisat/ASAR     | 2006 | Dec   | 29  |

Table 1. Dates of the Envisat data acquisitions used in the study.

Although clouds have a minor influence on the backscatter signal, we used the daily Moderate-Resolution Imaging Spectroradiometer (MODIS) Cloud Product for the extraction of the cloud spatial distributions in sampled areas during the radar data acquisition dates. As we know, radar signal propagate through clouds, however atmospheric gases dominated by oxygen and water vapour absorption could has influence on the backscatter signal [12].

We used DORIS software to focus raw Envisat ASAR data. We co-registered the SAR images based on the cross-correlation of the Single-Look Complex (SLC) data in an attempt to improve the multi-temporal backscatter analysis. The backscatter coefficients of the distributed targets were extracted from all SAR images (<https://earth.esa.int/handbooks/asar/CNTR2-11-5.html>). We applied a temporal filter and spatial averaging to the backscatter intensity to reduce speckle artifacts due to the sensor being unable to resolve individual scatters [4].

We then calculated a coherence map to detect random changes on land surface by measurement of temporal decorrelation. Coherence maps with proper spatial and temporal baselines between acquisitions were created using a

cross-correlation product derived from two co-registered complex values, both intensity and phase components [13]. We finally created twenty-seven coherence maps. To avoid a loss of coherence due to a geometrical deccorelation we used pairs of radar images with a short spatial baseline (65.3 m). To reduce a temporal decorrelation we choose a pair with a short temporal baseline (65 days). The coherence values are on the range from 0 to 1. Values close to 0 indicate a loss of coherence. In all calculations, layover and shadow effects, as well as the sea, were masked by using information from the DEM of the area.

## RESULTS

### Backscatter coefficient

We identified the mean backscatter coefficients of the five main land cover types in the area: sclerophyll, coniferous, wood-shrub, cultivated olive groves and farmland. Figure 2 presents the time series of the mean backscatter coefficients for each land cover type.

Wood-shrub areas show the lowest temporal backscatter coefficient variations from -11 to -9.5 dB presenting no clear seasonal pattern. Highest values are observed in 17 February 2005 and lowest in 8 April 2005. Coniferous show a temporal backscatter coefficient ranging from -9 to -8 dB. Highest values occur in 22 July 2005 and lowest values occur in 8 April 2005. There is no significant seasonal variation observed. Slightly higher values observed in summer could be due to the generation of new needles during this period (Fig. 2). Temporal changes of sclerophyll backscatter coefficient vary from -8 to -7.3 dB. The backscatter coefficient of sclerophyll reaches its highest values in winter (17 February 2006) or early spring (24 March 2006) time and the lowest in 8 April 2005 (Fig. 2). Wood-shrub and coniferous areas have a high vegetation density. The sclerophyll area is 60% covered by vegetation and has a higher backscatter coefficient than the other two aforementioned areas. Soil existence in sclerophyll area is important for the backscatter coefficient [8].

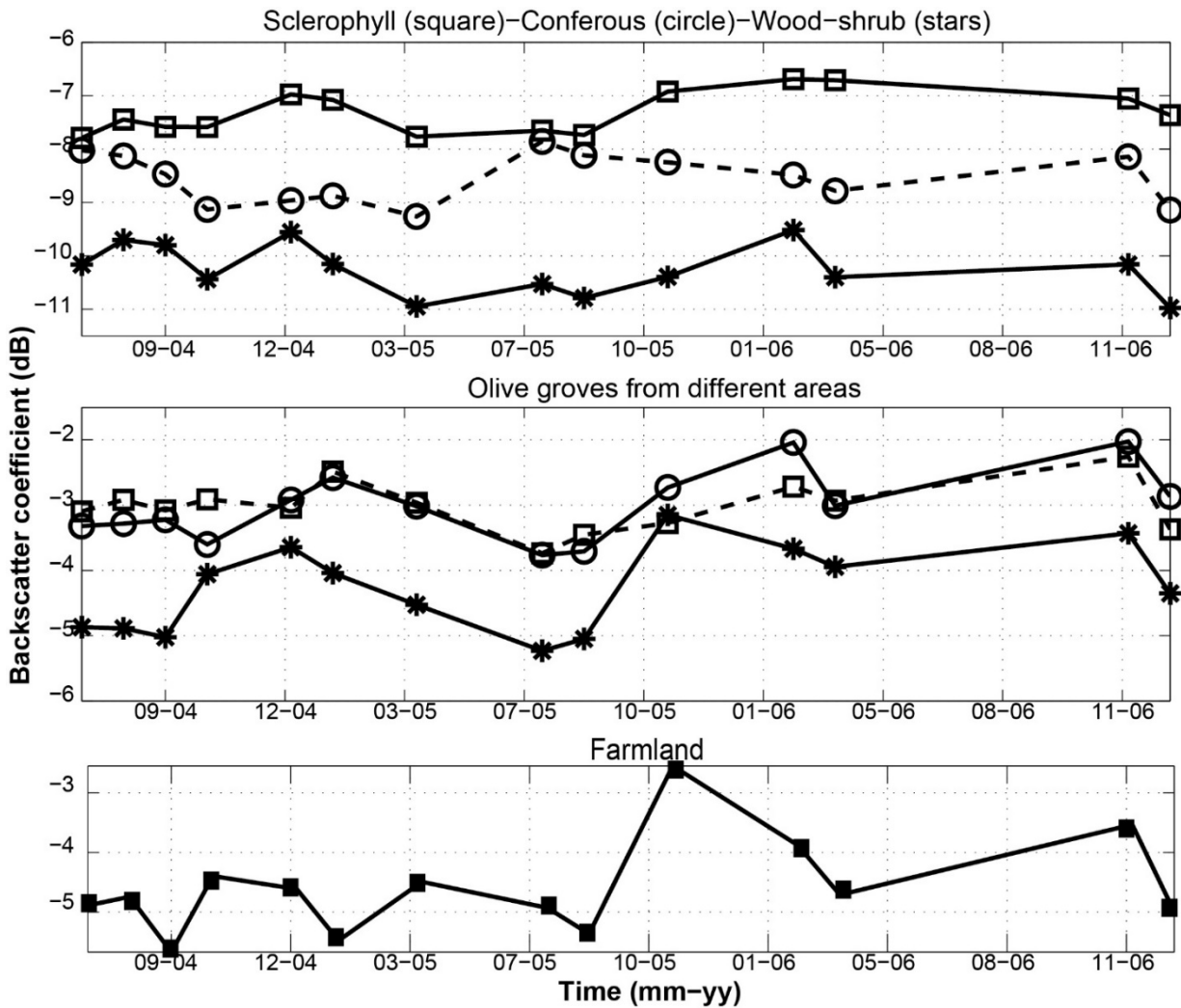


Figure 2. Backscatter coefficient plots. The first panel presents time series of the backscatter coefficients for the sclerophyll (square), coniferous (circle) and wood-shrub (stars). The second panel presents the time series of backscatter coefficients for the different olive groves. The bottom panel shows the variation of the backscatter coefficient for the farmland.

We also measured two olive grove areas, one of 58 m<sup>2</sup> surface (Fig. 2, olives plot, cycle and the other of 27m<sup>2</sup> (Fig. 2, olives plot, square)) are located close to each other (~2 km, Fig. 1). These areas consist approximately of 50 % olive trees and 50% soil. The variation of the backscatter coefficient for both is from -4 to -2 dB. Highest backscatter values are observed in 11 November 2006 and the lowest in 22 July 2005. A third olive grove area of 675 m<sup>2</sup> (Fig. 2, olives plot, stars) was selected located 18 km east of the other two olive groves (Fig. 1). The variation of the backscatter coefficient is from -5 to -3 dB. The observed relatively lower average backscatter coefficient variation compared to the aforementioned two olive groves could be due to a higher participation of soil surface roughness in

the backscatter. Such observations have been referred in literature by [14]. Changes in soil surface roughness conditions related to agricultural practice or to precipitation and wind effects can significantly change backscatter properties. The backscatter coefficients of all olive groves samples show maximum values in the end of autumn and winter (Fig. 2).

Farmland backscatter coefficients vary from -5.5 to -4 till October 2015. After October 2015, values raise to up to -3. Such variation pattern can occur due to a change in crop type in the farmland. However, for the whole period of study no clear seasonality pattern is observed. This could be explained by man activities such as watering, harvesting, tillage practices etc.

Precipitation can also affect the moisture content of vegetation and soil [15]. In terms of precipitation, precipitation it occurred only in one acquisition date (24 Dec 2004) (35.05mm). There was no precipitation in days, either during or before acquisitions.

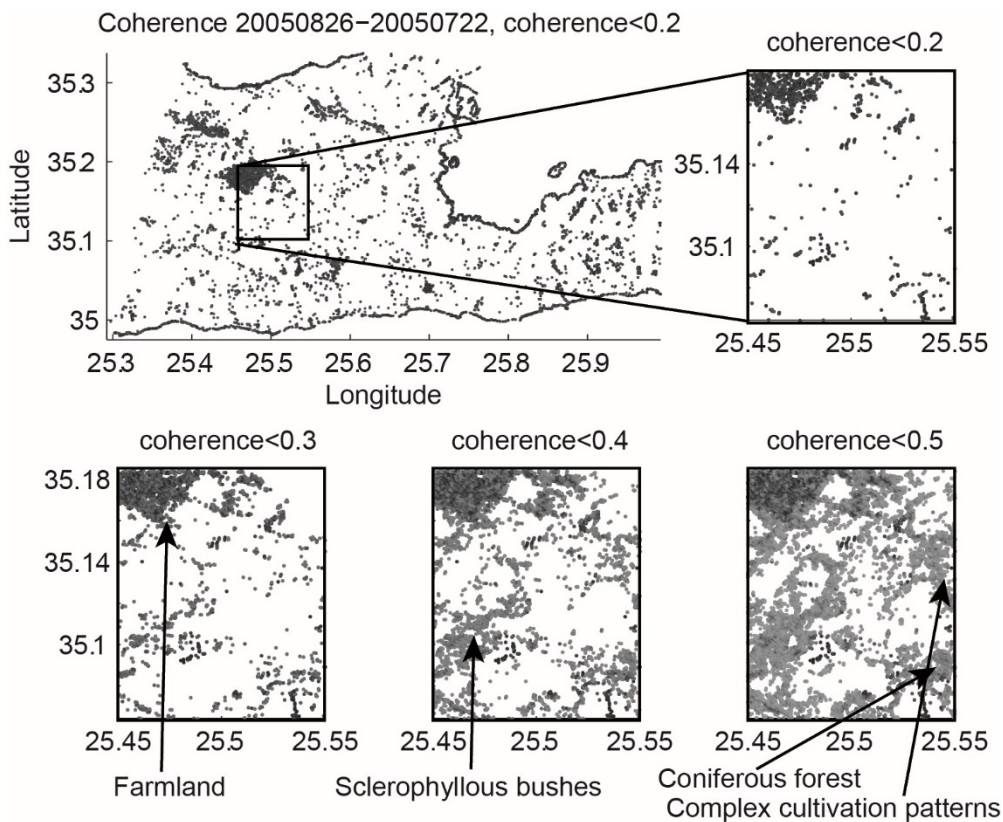


Figure 3. Coherence map between two acquisitions: 26 August 2005 and 22 July 2005. The spatial baseline is 65.3 m. Small panels present area in frame with different coherence threshold (grey colour). The grey colour indicates area with coherence values corresponding to a certain coherence threshold. The white colour indicates areas where no or not significant changes occurred (coherence close to 1). Different vegetation types have different ranges of the coherence values.

## Coherence

In Figure 3, the coherence map shows areas with loss of coherence (i.e. means coherence values  $< 0.3$ ). These correspond to farmlands or ravines with high density of wild olive groves mixed with farmland and/or cultivated olive trees (Fig. 3). However, when applying a coherence threshold of 0.15, i.e. observed coherence values lower than 0.15 correspond mostly to farmlands with probably high growth plant rates. Other dry and slow-growing vegetation types do not seem to affect significantly the coherence. However, the changes of coherence threshold reveal different type of vegetation (Fig. 3). For instance, the coherence values of the sclerophyllous bushes are in the range from 0.3 to 0.4 in the coherence map presented here. At the same time, the coherence values of the coniferous forest and complex cultivation patterns are in the range from 0.4 to 0.5. A coherence map with other spatial and temporal baselines could present different range of coherence values for these vegetation types.

## CONCLUSION

We investigated the potential of multi-temporal C-band SAR data for land cover discrimination. Mean backscatter coefficients and coherence map were calculated from SAR data. Using additional data, such as land cover maps, we extracted backscatter coefficients for different vegetation types and traced changes of backscatter coefficient in time. We also used MODIS data and meteorological records from a nearby ground station. However due to the dry weather during acquisition days we could not conclude in any connection of the backscatter coefficient with moisture.

We defined the range of the mean backscatter coefficients for each samples. The maximum fluctuation of the mean backscatter coefficient in time is no more than 2 dB. The maximum variation of the mean backscatter coefficients have the wood-shrub and olive groves samples. Probably, in these cases the backscatters at C-band is the sum of direct contribution from soil and the canopy itself [5].

All samples do not show strong seasonal trends. The backscatter coefficients of sclerophyll and olive groves samples show similar trend i.e. show low backscatter coefficient during summer and maximum one during winter. These samples consist approximately 40-50% of soil which could have an important impact to the backscatter and could explain the highest backscatter during winter and early spring time. However, to retrieve more conclusive results it is necessary to process longer time series and investigate complementarity with SAR data with different frequency and/or polarization characteristics.

Coherence shows to be effective in the detection of rapidly growing vegetation such as the farmland. Using different coherence thresholds other vegetation types can be extracted (Fig. 3) [16]. However, the loss of coherence can be attributed to different factors, such as geometric distortion and/or poor resolution. Other data sources (land cover, thematic map) could improve the coherence analysis for detection of different vegetation types [17]. In the case of short spatial and temporal baselines, coherence map may be potentially used to differentiate land cover types.

## ACKNOWLEDGEMENT

We acknowledge to European Space Agency for providing us ENVISAT data through research project ESA cat-1

6287.

## REFERENCES

- [1] A. Ferretti, A. Monti-Guarnieri, C. Prati, F. Rocca, and D. Massonnet, [InSAR Principles: Guidelines for SAR Interferometry Processing and Interpretation] Noordwijk: European Space Agency Publication, TM-19, (2007).
- [2] L. Zhong and D. Dzurisin, [InSAR Imaging of Aleutian Volcanoes: Monitoring a Volcanic Arc from Space] Springer Science & Business Media, (2014).
- [3] B. Biescas, E. Crosetto, M. Agudo, M. Monserrat, O., and Crippa, "Two Radar Interferometric Approaches to Monitor Slow and Fast Land Deformation," *J. Surv. Eng.* vol. 133, pp. 66–71 (2007).
- [4] J. M. Martinez and T. Le Toan, "Mapping of flood dynamics and spatial distribution of vegetation in the Amazon floodplain using multitemporal SAR data," *Remote Sens. Environ.* vol. 108, pp. 209–223 (2007).
- [5] S. Quegan, T. Le Toan, J. J. Yu, F. Ribbes, and N. Floury, "Multitemporal ERS SAR analysis applied to forest mapping," *IEEE Trans. Geosci. Remote Sens.* vol. 38, pp. 741–753 (2000).
- [6] M. Priess, D. Gray, and N. Stacy, "A change detection technique for repeat pass interferometric SAR," *IEEE International Geoscience and Remote Sensing Symposium. Proceedings (IEEE Cat. No.03CH37477)* vol. 2, pp. 938–940 (2003).
- [7] T. Mo, T. Schmugge, and T. Jackson, "Calculation of radar backscattering coefficient of vegetation-covered soil," *Remote Sens. Environ.* vol. 15, pp. 119–133 (1984).
- [8] Y. Wang, J. L. Day, and F. W. Davis, "Sensitivity of Modeled C- and L-Band Radar Backscatter to Ground Surface Parameters in Loblolly Pine Forest," *Remote Sensing of Environment* vol. 342, 331–342 (1998).
- [9] M. . Wooding, E. Attema, J. Aschbacher, M. Borgeaud, R. . Cordey, H. De Groof, J. Harms, J. Lichtenegger, G. Nieuwenhuis, C. Schmullius, and A. . Zmuda, "Satellite radar in agriculture: experiences with ERS-1," *ESA Publ. Div.* vol. SP-1185, (1995).
- [10] A. Ferretti, C. Prati, and F. Rocca, "Permanent scatterers in SAR interferometry," *IEEE Trans. Geosc. Remote Sensing.* 39, 8-20 (2001).
- [11] R. F. Hanssen, [Radar Interferometry: Data Interpretation and Error Analysis] Kluwer Academic Publishers, Dordrecht, (2001).
- [12] Y. Kinoshita, M. Shimada, and M. Furuya, "InSAR observation and numerical modeling of the water vapor signal during a heavy rain: A case study of the 2008 Seino event, central Japan," *Geophys. Res. Lett.* vol. 40, pp. 4740–4744 (2013).
- [13] H. A. Zebker and J. Villasenor, "Decorrelation in interferometric radar echoes," *IEEE Geosci. Remote Sens.* vol. 30, pp. 950–959 (1997).
- [14] P. Marzahn and R. Ludwig, "On the derivation of soil surface roughness from multi parametric PolSAR data and its potential for hydrological modelling," *Hydrol. Earth Syst. Sci.* vol. 13, pp. 381–394(2009).

- [15] Z. Lu and D. . Meyer, "Study of high SAR backscattering caused by an increase of soil moisture over a sparsely vegetated area: implications for characteristics of backscatter," *Int. J. Remote Sens.* vol. 23, pp. 1063–1074 (2002).
- [16] U. Wegmuller and C. Werner, "Retrieval of vegetation parameters with SAR interferometry," *IEEE Trans. Geosci. Remote Sens.* vol. 35, pp. 18–24 (1997).
- [17] J. G. Liu, H. Lee, and T. Pearson, "Detection of rapid erosion in SE Spain: a GIS approach based on ERS SAR coherence imagery," *Remote Sensing for Earth science, ocean and sea ice App.* vol. 3868, pp. 525–535 (1999).